ABCM Symposium Series in Mechatronics - Vol. 4 - pp.700-709

A SPECIALIZED WELDING ROBOT FOR REPAIRING HYDRAULIC TURBINE BLADES

José Maurício S. T. Motta, jmmotta@unb.br
Guilherme Caribé de Carvalho, gccarval@unb.br
Carlos Humberto Llanos Quintero, llanos@unb.br
Walter de Britto Vidal Filho, wbritto@unb.br
Enio Prates Vasconcelos Filho, enioprates@yahoo.com.br
Universidade de Brasília, Faculty of Technology, Mechanical Engineering Department
70.910-900, Brasilia – DF, Brazil
Luciano Selva Ginani, luciano.ginani@tu-ilmenau.de
Technische Universität Ilmenau, Faculty of Mechanical Engineering
P.O. Box 10 05 65
98684 Ilmenau, Germany

Abstract. *The article presents the steps of a R&D project aiming at designing and constructing a specialized welding robotic system for recovering material damage on hydraulic turbine blades. The current project proposes a methodology and presents the construction steps of a robotic prototype to automate the welding process with the purpose of repairing hydraulic turbine blades eroded by cavitation pitting and/or cracked by cyclic loading, reducing human risks and increasing the efficiency of the process. Hydraulic turbines installed in hydroelectric plants are subject to several types of mechanical wearing. The sources of mechanical straining can range from operational conditions of the hydro generator, poor design characteristics, properties of the blade material employed and operation points out of specification as a consequence of overloading. An established process for repairing the surface of turbine blades eroded by cavitation or damaged by fatigue cracks is to recover the material flaws by using electric arc welding. The welding process is carried out manually after visual inspection of the blade surface, requiring a halt of the turbine. This is a very harsh human labor condition, in air temperatures around 40°C and 99% of air humidity for tenths of hours. The robotic system proposed has a spherical topology with 5 degrees of freedom, electric stepper motors, rotary and linear actuators and a 2.5m-diameter workspace. The system has an embedded measurement system with a vision sensor especially built to produce range images by scanning laser beams on the blade surface. The range images are used to construct 3-D models of the blade surface and the location of the damaged spots are recorded into the robot controller in 3-D coordinates, thus enabling the robot to repair the flaws automatically by welding in layers. The measurement vision system accuracy was assessed to be about 1:1000 when compared to the distance from the measured surface. The robot controller and measurement system are built in FPGA based reconfigurable microprocessors. The welding process is the GMAW (Gas Metal Arc Welding) using a composite GMAW electrode (tubular metal cored electrode) carried out with a pulsed GMA welding machine. The robotic system was designed to have high rigidity mechanics, easy assembly and fixing on the blade surface and hassle-free operation. Low cost, light weight, portability, high positioning accuracy and repeatability are also characteristics of the resulting robotic system.*

Keywords*: Welding Robot; Turbine Blades Defects; Special Robots; Robotized Welding*

1. INTRODUCTION

The article presents the steps of a R&D project aiming at designing and constructing a specialized welding robotic system for recovering material damage on hydraulic turbine blades. The current project proposes a methodology and presents the construction steps of a robotic prototype to automate the welding process with the purpose of repairing hydraulic turbine blades eroded by cavitation pitting and/or cracked by cyclic loading, reducing human risks and increasing the efficiency of the process.

Hydraulic turbines installed in hydroelectric plants are subject to several types of mechanical wearing. The sources of mechanical straining can range from operational conditions of the hydro generator, poor design characteristics, properties of the blade material employed and operation points out of specification as a consequence of overloading (Parmar, 1997, Ecober et al., 2006).

The most common cause of rotor wearing is the erosion by cavitation pitting (Hammit, 1979, Amdt, 1981). This is a highly undesirable phenomenon in the operation of a turbine. The water that flows through the turbine ducts during operation generates pressure fields on the blade surface that can be below the water vapor pressure in the operation temperature. This extreme operation condition generates vapor bubbles that can be collapsed when they reach regions of abrupt changes in pressure and flow conditions. When such bubbles collapse, they produce high shock pressure waves, which cause tearing out of bits of metal when the collapse occurs in adjacent regions of the runner blades (Fig. 1). This cyclical loading of high amplitude produces fatigue erosion on the blade surface, causing substantial loss of material

(Li, 2000). Fatigue cracks are more rarely found, but the phenomenon can happen in hardened steels, such as martensitic stainless steels.

An established process for repairing the surface of turbine blades eroded by cavitation or damaged by fatigue cracks is to recover the material flaws by using electric arc welding. The welding process is carried out manually after visual inspection of the blade surface, requiring a halt of the turbine. This is a very harsh human labor condition, in air temperatures around 40°C and 99% of air humidity for tenths of hours.

Figure 1- Hydraulic turbine blades damaged by cavitation.

This project is intended to improve the quality of cavitation damage repairs in hydraulic turbine blades using robotic welding, reducing welding defect rates, material consumption, time-to-repair and overall repairing costs. Besides, the proposed technology can remove weld personnel from harsh environment, achieve a better blade profile and improve weld consistency.

3. ROBOT DESIGN

For a robot to realize all tasks needed in the application proposed it has to be able to fulfill the requirements below:

a) capacity to operate in any position: horizontal, vertical or inverted; b) low weight: portability and fixation to the blades; c) rigidity to deflection: load on wrist occurs in any direction and arm extension; d) high motion accuracy: capacity to reach accurately welding regions from the mapped geometry; e) availability of parts in the market; f) control with component interfacing capability; g) topology making feasible to measure large areas with laser scanning and 3d geometry mapping; h) large workspace; i) easiness to be fixed to the turbine blades.

The robotic system proposed has a spherical topology with 5 degrees of freedom, electric stepper motors, rotary and linear actuators and a 2.5m-diameter workspace. The system has an embedded measurement system with a vision sensor especially built to produce range images by scanning laser beams on the blade surface. The range images are used to construct 3-D models of the blade surface and the location of the damaged spots are recorded into the robot controller in 3-D coordinates, thus enabling the robot to repair the flaws automatically by welding in layers. The robot controller and measurement system are built in FPGA-based reconfigurable microprocessors. The welding process is the GMAW (Gas Metal Arc Welding) using a composite GMAW electrode (tubular metal cored electrode) carried out with a pulsed arc welding machine.

The robotic system was designed to have high rigidity mechanics, easy assembly and fixing on the blade surface and hassle-free operation. Low cost, light weight, portability, high positioning accuracy and repeatability are also characteristics of the resulting robotic system.

The proposed robot has the following capacities:

a) spherical topology with 5 degrees-of-freedom, 3 in the manipulator (2 rotation and 1 translation) and 2 (rotation) in the wrist; b) surface mapping with only one scanning pass; c) embedded electronics; d) GMA Welding; e) fixation on blades by magnetic devices or by air suction (still to be defined); g) construction by assembling off-the-shelf parts, allowing construction of several low-cost prototypes using an assembly manual; i) low cost and time to design.

3. THE PROTOTYPE CONSTRUCTED

The robot was assembled using off-the-shelf parts found in the international market and each part was selected according to the needs and design criteria related to high rigidity to deflection, high positioning accuracy, low weight, large workspace but with short dimensions vertically to be easily inserted between blades. All parts were constructed and assembled using CAD software and the drawings can be viewed in Fig. 2:

The robot constructed has a weight of 30kg, a ring-shaped workspace of 2.5m outer diameter x 60cm height and dimensions of (30 x 25 x 100cm), without the welding torch.

The manipulator is conceived to carry an integrated control system to manage various tasks and may be considered an intelligent robot, since those tasks can be executed without human action. The control system is designed such that, after receiving from the operator the delimitation of the surface area to work, it manages the robot actions to recognize

the environment, to extract the location and the volume of material to be filled, to determine the strategies for slicing the volume into a sequence of weld beads, to generate trajectories to be followed by the welding torch, and to control the robot movements during the welding tasks and during the change of torch positions defined by the slicing strategy.

Figure 2 – Robot prototype assembled and compared with the turbine model.

All of these actions are carried out without further external stimulation. Figure 3 presents a simplified block diagram of the modules of the robot control system.

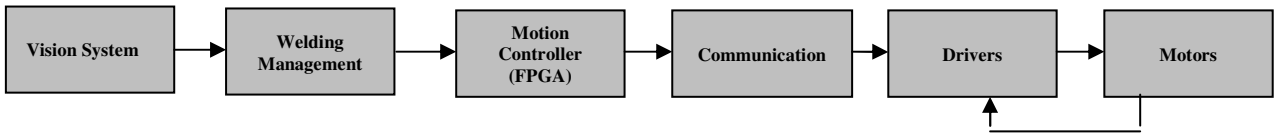

Figure 3. Robot Control Modules

a) **Vision system module:** it is responsible for mapping the surface geometry on which the robot is to weld. The vision sensor scans the turbine blade surface and generates cloud points in 3D coordinates (Ginani, 2007) that have to be represented further in robot coordinates, recognizing by image processing and pattern recognition algorithms which parts are damaged and the original blade profile to be recovered.
b) **Welding Management Module:** this module receives data from the vision sensor with areas to be welded as well as their 3D geometry. With the areas and volumes to be welded and knowing the expected geometry of the welding beads, which have been previously modeled as a function of the welding parameters, this module calculates the correct slicing strategy to recover the original geometry by welding parallel weld beads in each plan to be superimposed. This module is also responsible for selecting a welding procedure, from a previously defined data base, as a result of the measured relative direction between the gravity vector and the average normal vector to the original surface, thus setting the welding parameters on the welding power source, as well as defining the start and end points of each weld bead.
c) **Motion Control Module:** controls the motion of the electric motors according to the robot kinematic model. The welding manager sends the list of the target positions to be welded through a RS232 interface to the motion controller, which is responsible to generate the right commands to the power drivers in order to move the manipulator. The implementation of the motion control model in FPGA allows more flexibility and efficiency in it, as well as allowing rapid changes in the motion control hardware, as for example, the addition of more processors, hardware accelerators or modules for arithmetic operations. The motion control is based on an open loop feedforward speed control strategy with encoder position feedback for the wrist axes. A block diagram for the control strategy can be viewed in Figure 4.
d) **Communication Module:** For the communication between the control module and the electric motors, two communication lines were implemented, one using digital signals for controlling the first 3 robot axes, which are driven by step frequency and direction signals, and the other based on a standard RS485 network, which is used to

transmit movement commands and data to and from the driver that controls the 2 orientation axes at the robot wrist. The control module sends the motion commands to the wrist motors via a RS232 port, which is connected to the network by a RS232-RS485 converter, whereas the motion commands to the first three axes are sent via dedicated FPGA digital output lines. This strategy was adopted since it would guarantee the necessary synchronism among the first three axes, which do not have position feedback. The synchronism of these and the two orientation wrist axes is attained by using a position feedback from encoders installed in each wrist axis and a different control cycle frequency. Such a strategy also facilitates the communication between the robot controller and other controllers present on the site, such as the welding power source. Each controller associated to a network node has an identification address, allowing commands to be sent to all nodes by broadcasting. Each controller identifies its specific commands by analyzing the address associated with each command launched on the network.

e) Motors and Drivers Module: This module includes the five electric motors, their controllers and drivers.

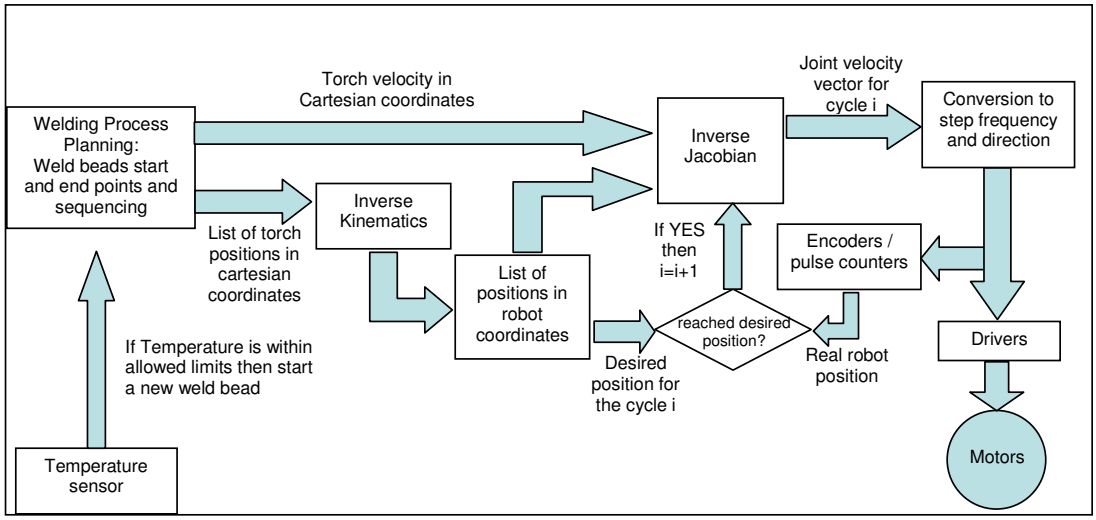

Figure 4 – Robot control scheme

4. MEASUREMENT VISION SENSOR

The built-in vision sensor is based on laser scanning and active triangulation for dense surface acquisition and construction of 3-D models of the blade surface. In order to design a vision sensor capable of mapping the blade surface with high speed and accuracy, three main aspects were considered: sensor structure, image processing and calibration. The sensor structure defines the triangulation parameters and equations; image processing detects the laser stripes and samples them, thus generating the input data for the triangulation equations; and calibration solves the sensor parameters and is a critical procedure for the measurement accuracy.

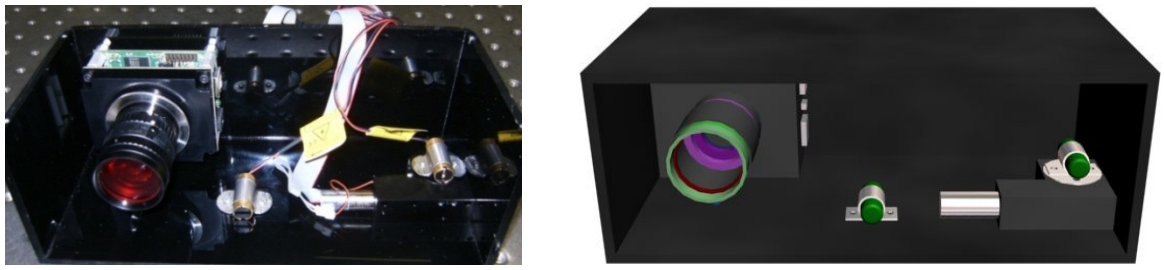

Figure 5: Vision Sensor Design

The vision system is composed by a high resolution USB black and white camera (1616x1216 pixels), 2 laser diodes (7mW) with stripe projection lens and a controlled rotary actuator for one laser diode (stepper motor) (Fig. 5). The system does not need any angular position encoder. The geometrical relation between the laser planes and the camera is determined by the sensor structure and can be mathematically modeled as in Fig. 6.

The equations relating camera coordinates with the 3D world coordinates of the object target can be seen in Eqs. (1) and (2) , where *f, bx, by, dy and dx* have to be previously calibrated using a precision plate marked with white dots on a black board and the camera model.

So, since (x_{int}, y_{int}) is the intersection between the two laser stripes projected on the object surface (Fig. 7) it is possible to calculate the range image (3D coordinates) of the object using Eqs. (2) and (3).

Thus, with a direct relation between image coordinates of the laser stripe retrieved from the image by using image processing and the object 3-D camera coordinates, it is possible to reconstruct the damaged blade surface.

$$\begin{bmatrix} x_c \\ y_c \\ z_c \end{bmatrix} = \frac{b_x'}{f\cot(\theta_x) + x_u} \begin{bmatrix} x_u \\ y_u \\ f \end{bmatrix} \qquad \begin{bmatrix} x_c \\ y_c \\ z_c \end{bmatrix} = \frac{b_y'}{f\cot(\theta_y) + y_u} \begin{bmatrix} x_u \\ y_u \\ f \end{bmatrix} \tag{1}$$

$$\begin{cases} \cot(\theta_y) = \frac{1}{f}\left[\frac{b_y}{b_x}(f\cot(\theta_x) + x_{int}) - y_{int}\right]\left[1 - \frac{d_y}{fb_x}(f\cot(\theta_x) + x_{int})\right]^{-1} \\ \cot(\theta_x) = \frac{1}{f}\left[\frac{b_x}{b_y}(f\cot(\theta_y) + y_{int}) - x_{int}\right]\left[1 - \frac{d_x}{fb_y}(f\cot(\theta_y) + y_{int})\right]^{-1} \end{cases} \tag{2}$$

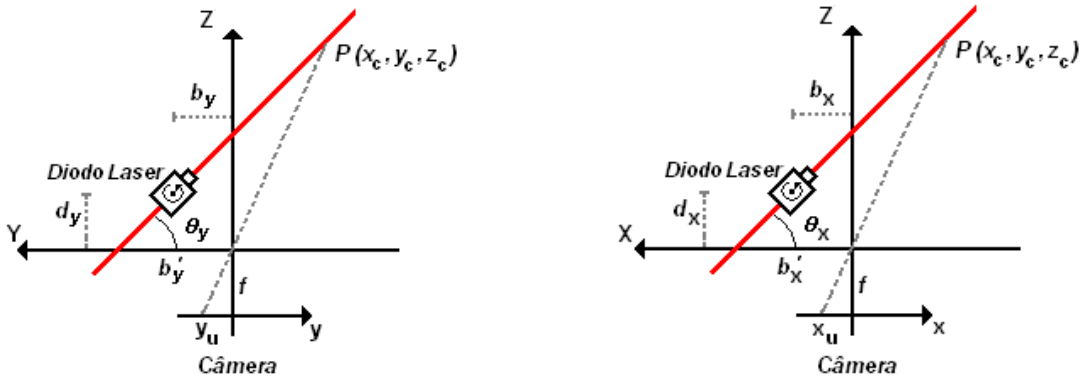

Figure 6: Vision Sensor Mathematical Model

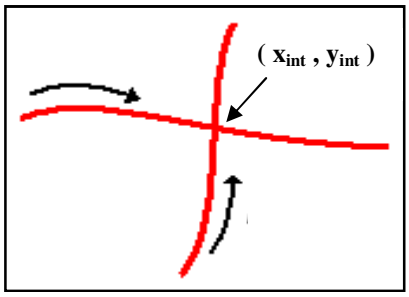

Figure 7. Intersection of the laser stripes.

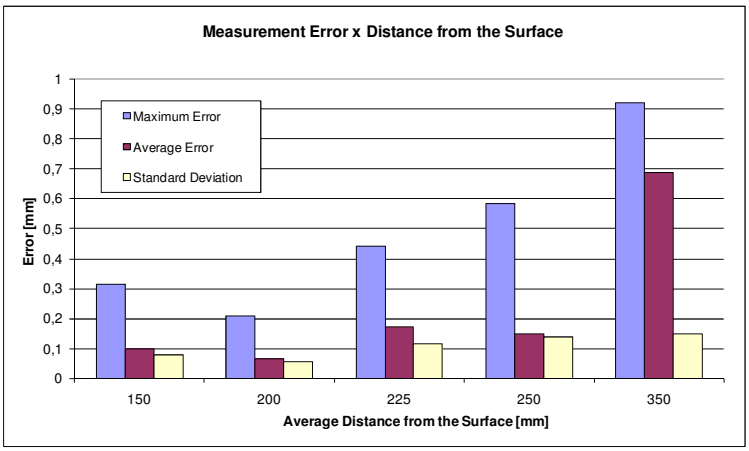

Figure 8 – Assessment of the position accuracy when measuring the 3-D dimensions of a standard block with 50mm width in several orientations.

ABCM Symposium Series in Mechatronics - Vol. 4 - pp.700-709

Whilst one of the laser planes is used for surface reconstruction, sweeping the whole surface while θy changes, the second laser plane is used solely for calculation of the sweeping angle with a higher accuracy then by using encoders, thus improving the stand-off distance in which the system can operate. An assessment of the vision system accuracy can be seen in Fig. 8.

4. KINEMATIC MODEL AND CALIBRATION

A robot can be modeled as a series of links connecting its end-effector to its base, with each link connected to the next by an actuated joint.

Robot construction by assembling modular off-the-shelf parts brings about flexibility in manufacturing and allows the construction of several prototypes in the shop-floor, but also produces many sources of assembling inaccuracies. So, in order to achieve the desired accuracy, it is essential to calibrate each robotic system model to fit all the geometrical uncertainties. Besides, it is never possible to measure distances and angles between joints when there is no access to internal parts where the joint coordinate frames have to be assigned to represent the robot actual motion.

Robot calibration is an integrated process of modeling, measurement, numeric identification of actual physical characteristics of a robot, and implementation of a new model that describes more precisely the robot. (Schröer, 1993).

The joint coordinate frames have to be assigned by using a rational convention, associated to a zero position (where all joint variables are set to zero). So, it is assumed that for the assignment of coordinate frames to each link the manipulator has to be moved to its zero position. The zero position of the manipulator is the position where all joint variables are zero. This procedure may be useful to check if the zero positions of the model constructed are the same as those used by the controller, avoiding the need of introducing constant deviations to the joint variables (joint positions).

Subsequently the z-axis of each joint should be made coincident with the joint axis. This convention is used by many authors and in many robot controllers (McKerrow, 1995, Paul, 1981). For a prismatic joint, the direction of the z-axis is in the direction of motion, and its sense is away from the joint. For a revolute joint, the sense of the z-axis is towards the positive direction of rotation around the z-axis. The positive direction of rotation of each joint can be easily found by moving the robot and reading the joint positions on the robot controller display.

According to McKerrow (1995) and Paul (1981), the base coordinate frame (robot reference) may be assigned with axes parallel to the world coordinate frame. The origin of the base frame is coincident with the origin of joint 1 (first joint). This assumes that the axis of the first joint is normal to the x-y plane. This location for the base frame coincides with many manufacturers' defined base frame.

Afterwards coordinate frames are attached to the link at its distal joint (joint farthest from the base). A frame is internal to the link it is attached to (there is no movements relative to it), and the succeeding link moves relative to it. Thus, coordinate frame i is at joint i+1, that is, the joint that connects link i to link i+1.

The origin of the frame is placed as following: if the joint axes of a link intersect, then the origin of the frame attached to the link is placed at the joint axes intersection; if the joint axes are parallel or do not intersect, then the frame origin is placed at the distal joint; subsequently, if a frame origin is described relative to another coordinate frame by using more than one direction, then it must be moved to make use of only one direction if possible. Thus, the frame origins will be described using the minimum number of link parameters.

The x-axis or the y-axis have their direction according to the convention used to parameterize the transformations between links. At this point the homogeneous transformations between joints must have already been determined. The other axis (x or y) can be determined using the right-hand rule.

A coordinate frame can be attached to the end of the final link, within the end-effector or tool, or it may be necessary to locate this coordinate frame at the tool plate and have a separate hand transformation. The z-axis of the frame is in the same direction as the z-axis of the frame assigned to the last joint (n-1).

The end-effector or tool frame location and orientation is defined according to the controller conventions. The robot nominal kinematic model can be seen in Fig. 9.

There are many desirable characteristics for a kinematic model, but when considering kinematic models constructed aimed at using in robot calibration procedures three are mostly important: completeness, continuity and minimality (Motta, 2005; Albright, S.L., 1993). Completeness is the ability of a kinematic model to describe all possible spatial geometric joint configurations of a robot. Continuity and minimality influence directly robot calibration, since they are related to model smoothness and to parameter redundancies in the model respectively.

Robot kinematic models are generally based on the Denavit-Hartenberg convention (McKerrow, J.P., 1991) because of its simplicity and easiness to be geometrically represented. The elementary transformations can be formulated as:

Denavit-Hartemberg convention $$T = f(\theta, \alpha, d, l) = R_Z(\theta)T_Z(d)T_X(l)R_X(\alpha) \quad (3)$$

, where T represents position and orientation coordinates of a link frame related to a previous one, where θ and α are the rotation parameters, *d* and *l* are translation parameters.

ABCM Symposium Series in Mechatronics - Vol. 4 - pp.700-709

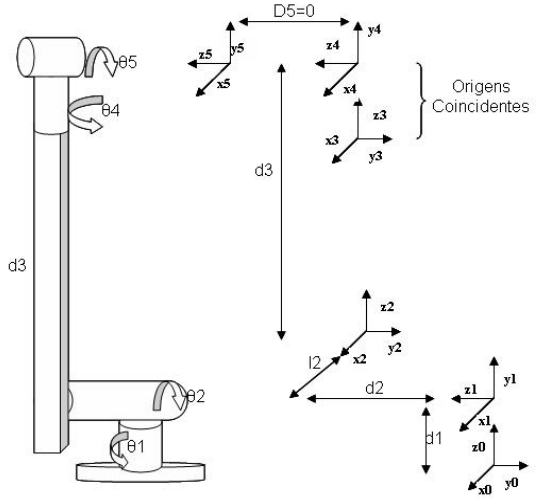

Figure 9: Schematics of the robot kinematic model

However, when considering an error parameter model for robot calibration a single minimal modeling convention that can be applied uniformly to all possible robot geometries cannot exist owing to fundamental topological reasons concerning mappings from Euclidean vectors to spheres (Schröer, 1993). However, after investigating many topological problems in robots, concerning inverse kinematics and singularities, Baker (1990) suggested that the availability of an assortment of methods for determining whether or not inverse kinematic functions can be defined on various subsets of the operational spaces would be useful, but even more important, a collection of methods by which inverse functions can actually be constructed in specific situations. An insightful paper about robot topologies was published by Gottlieb (1986), who noted that inverse functions can never be entirely successful in circumventing the problems of singularities when pointing or orienting.

Mathematically, model-continuity is equivalent to continuity of the inverse function T^{-1}, where T is the product of elementary transformations (rotation and translation) between joints. From this, the definition of parameterization's singularity can be stated as a transformation $Ts \in E$ (parameterization's space of the Euclidean Group - 3 rotations and 3 translations), where the parameter vector $p \in R^6$ (p represents distance or angle) exists such that the rank of the Jacobean Js = dTs/dp is smaller than 6. In other way, each parameterization T can be investigated concerning their singularities detecting the zeroes of determinant $\det(J^T.J)$ considered as a function of parameter p.

The robot (Fig. 9) has perpendicular and parallel axes. However, the Denavit-Hartemberg convention, shown in Eq. (3), cannot be used in error parameter models when modeling parallel axes due to singularities that occur in the Jacobean matrix, as explained. This matrix will be described ahead in the text in Eq. (4). This issue is discussed in details in Motta (2005) and Schröer (1997). A possible convention for parallel axes is the Hayati-Mirmirani, which cannot be used in perpendicular axes for the same reason. The Hayati-Mirmirani is as four-parameter convention that describe the transformation between two parallel axes as shown in Eq. (4).

$$\text{Hayati-Mirmirani convention} \quad f(\theta,\alpha,\beta,l) = R_Z(\theta)T_X(l)R_X(\alpha)R_Y(\beta) \tag{4}$$

Using the previous two conventions (Denavit-Hartemberg and Hayati-Mirmirani) and taking into account the requirements of a kinematic model (completeness, continuity and minimality), the singularity-free approach discussed was applied for the assignment of coordinate frames and for the definition of which error parameters should be included in the kinematic model (Motta, 2005). Using this approach a kinematic model representing mathematically this robot was constructed. The parameters used are shown in Table 1, where δ are the error parameters between the nominal model and the actual robot model to be identified by the calibration system, and are initially set to null.

Table 1: Kinematic parameters to be calibrated

Joints		**Parameters**					
From (type of joint)	**To** (type of joint)	**Tx**	**Ty**	**Tz**	**Rx**	**Ry**	**Rz**
Base (Base)	**Joint 1** (Rotation)	0+δ	0+δ	0	0°+δ	0°+δ	0°
Joint 1 (Rotation)	**Joint 2** (Rotation)	0+δ	0	110+δ	90°+δ	0°	0°+δ
Joint 2 (Rotation)	**Joint 3** (Prismatic)	30	0	−100	−90°+δ	0°	90°+δ
Joint 3 (Prismatic)	**Joint 4** (Rotation)	0+δ	0+δ	570	0°+δ	0°+δ	0°
Joint 4 (Rotation)	**Joint 5** (Rotation)	0+δ	0	0+δ	90°+δ	0°	0°+δ
Joint 5 (Rotation)	**TCP** (TCP)	0+δ	0+δ	0+δ	0°+δ	0°+δ	0°+δ

ABCM Symposium Series in Mechatronics - Vol. 4 - pp.700-709

From the mathematical point of view, robot calibration is a non-linear parameter estimation process. That means, a mathematical model to identify unknown parameters from experimental data by using a proper cost function to minimize errors.

A robot kinematic model can be seen as a function that relates kinematic model parameters and joint variables to coordinate positions of the robot end-effector. As an example to present the mathematics involved, a kinematic model following the Denavit-Hartenberg convention can be derived as (from Eq. (3)):

$$\Delta P = \partial P/\partial\theta \Delta\theta + \partial P/\partial\alpha \Delta\alpha + \partial P/\partial d \Delta d + \partial P/\partial l \Delta l \tag{5}$$

where P represents position and orientation coordinates of the manipulator end-effector (Tool Center Position – TCP) and θ, α, d and l are the four parameters that define the transformation from a robot joint frame to the next joint frame, where θ and α are the rotation parameters, d and l are translation parameters.

The first derivative of Eq. (3) can be interpreted as the position and orientation error equation of the robot TCP coordinates (Hollerbach, J.M. & Benett, D.J., 1988), where ΔP is the pose error and it can be physically measured.

Considering the manipulator transformation, P, from the robot's base frame to the TCP-frame, the measured robot position, M, related to the measurement system coordinate frame and the transformation that locates the robot base frame to the measurement system, B, (the transformation B have to be considered as a link that makes part of the robot model) then ΔP is the vector to be calculated in

$$\Delta P = M - P \tag{6}$$

The transformation P is then iteratively modified when the error parameters of the robot model are updated, and by the end of the calibration process the transformation P represents the actual robot and its location in the measurement system coordinate frame.

Rewriting Eq. (5) in a matricial form for various measured positions and orientations of the robot end-effector, Eq. (6) can be formulated as the Jacobean matrix containing the partial derivatives of P such as Δx is the vector of the model parameter errors,

$$\begin{bmatrix} \Delta P_1 \\ \Delta P_2 \\ \vdots \\ \Delta P_n \end{bmatrix} = \begin{bmatrix} \partial P_1/\partial\theta & \partial P_1/\partial\alpha & \partial P_1/\partial d & \partial P_1/\partial l \\ \partial P_2/\partial\theta & \partial P_2/\partial\alpha & \partial P_2/\partial d & \partial P_2/\partial l \\ \vdots & \vdots & \vdots & \vdots \\ \partial P_n/\partial\theta & \partial P_n/\partial\alpha & \partial P_n/\partial d & \partial P_n/\partial l \end{bmatrix} \begin{bmatrix} \Delta\theta \\ \Delta\alpha \\ \Delta d \\ \Delta l \end{bmatrix} = \begin{bmatrix} J_1 \\ J_2 \\ \vdots \\ J_n \end{bmatrix} \Delta x \Rightarrow \mathbf{J}\Delta x = \mathbf{\Delta P} \tag{7}$$

Thus the calibration problem is reduced to the solution of a non-linear system of the type Ax = b.

There are many different methods to solve this type of system and one of those that is widely used is the Squared Sum Minimization (SSM). Many authors (Jacoby, S.L.S. et al, 1972 ; Dennis, J.E. & Schnabel, R.B., 1983) discuss extensively those methods and algorithms are easily found in the literature (Press, W.H. et al, 1992).

One method to solve non-linear least-square problems that proved to be very successful in practice and thus recommended for general solutions, is the algorithm proposed by Levenberg-Marquardt (LM algorithm) (Dennis, J.E. & Schnabel, R.B., 1983). Several algorithms versions of the L.M. algorithm have been proved to be successful (globally convergent). It turns to be an iterative solution method by introducing few modifications in the Gauss-Newton method in order to overcome some divergence problems. (Jacoby, S.L.S. et al, 1972).

Since the geometric parameters of the robot model has been identified in the calibration model, two kinematic models are available, i.e. the nominal kinematic model and the calibrated model. The calibrated model cannot be inverted with explicit variables, since there are more geometric parameters (different of zero) than the nominal one. The solution for correcting the robot coordinates from a set of joint variables is position compensation.

5. THE ROBOT CONTROLLER

The robot controller is built with reconfigurable architectures (Field Programmable Gate Arrays). FPGA's are programmable logic devices that permit the implementation of digital systems. They provide arrays of logical cells that can be configured to perform given functions by means of configuration bitstream. The bitstreams are generated by a software tool, and usually contains the configuration information for all the components. Configuration of the FPGA can be realized by using several design/synthesis tools provided by companies such as Altera (2008) and Xilinx (2008). The circuit can be described using a high level description language as VHDL or Verilog (Becker and Hartenstein,

2003). The tool makes the synthesis of the description file producing a binary configuration file (bitstream file). This file is used to configure the FPGA device.

FPGAs permit to implement algorithm directly in hardware instead of in software (for instance, using microcontrollers). Implementation in software has limitations due to the sequential nature of von Newmann architectures that run the software model. In contrast, in FPGA implementations the potential of parallelism can be explored in order to improve the performance of the system. Moreover, the flexibility of these devices permits to configure (reconfiguration operation) the system even in real time. Reconfigurable systems are composed of a microcontroller and a FPGA working jointly. In this case one part of the system can be running in software (in the microcontroller) whereas the other part can be implemented in hardware (in the FPGA). In general, reconfigurable systems can be designed using hardware-software co-design approach which specifies methodologies in order to determine the system parts being implemented in software and hardware. This partitioning can be made taking into account a function cost that tries to optimize some circuit characteristic such as area, performance and power consumption of the system.

Figure 10 describes the overall architecture of the robot controller, which is composed of an FPGA embedded microprocessor (such the NIOS), an embedded bus (e.g. the Avalon bus) and other modules. The memory module is used for storing a supervisory program that is connected to the main bus jointly with the kinematics and dynamics controller modules. Differently of other proposed approaches (Kung et. Al. , 2006), the kinematics and dynamics modules are capable to implement float point operations directly in hardware. Trigonometric operations such as tangent, sine, among other are implemented using the IC algorithms (Andraka, 1998).

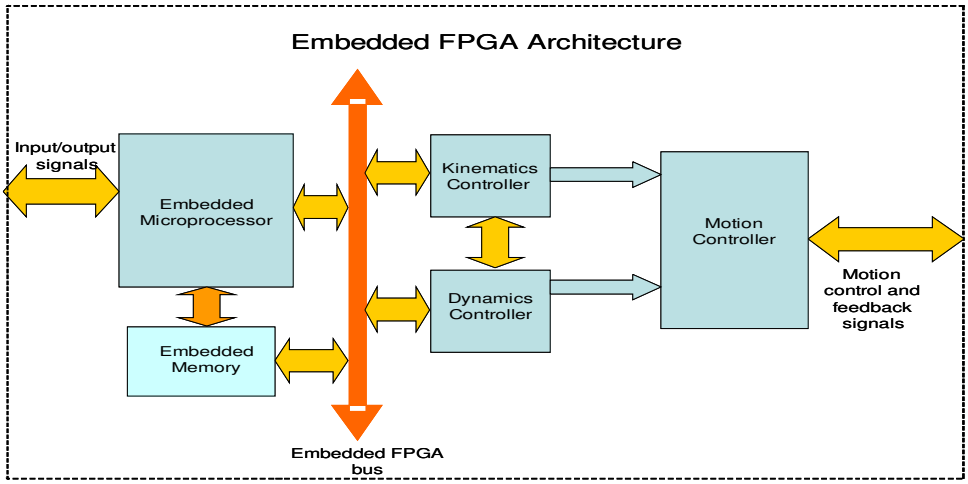

Figure 10. The overall FPGA embedded architecture for the robot controller

5. CONCLUSIONS

This article presented a research project that involves several topics related to mechanical engineering and mechatronics. The robot kinematics and calibration, control systems, vision sensor and hardware implementation are discussed.

The robot was designed to be used with an open loop control positioning system, relying on the accuracy of a vision sensor conceived to map the turbine blade three-dimensional surface and to detect their geometric defects for welding tasks. Robots positioning open loop controls require high accuracy in the determination of the robot geometrical parameters, since the coordinate systems of both sensor and robot must be referenced in a single system to allow automatic joint position programming based on 3D surface maps. This type of operation is equivalent to off-line robot programming, since it is not possible to correct robot positioning using the sensor in on-line operation. However, the system was designed to operate automatically.

Details of the vision sensor and their hardware were presented and discussed with experimental results showing that the system has sufficient accuracy for welding tasks. The most sensitive parameters on measurement accuracy have been identified and a more accurate system is currently being designed.

The robot calibration model was presented and discussed in the form of procedures that can be used with any robot calibration modeling. Experimental results are not yet available.

The robot is currently already operational, but the vision sensor and kinematic models still have to be integrated and calibrated. The control systems are fully implemented in embedded FPGA boards with much higher processing speed than common general purpose microprocessors.

6. ACKNOWLEDGEMENTS

ELETRONORTE (Electrical Power Plants of the North of Brazil) and FINATEC (Scientific and Technological Enterprises Foundation) are thanked for their financial support and collaboration. Our gratitude is especially conveyed to the staff of ELETRONORTE for their technical support and interest.

7. REFERENCES

Albright, S.L., 1993, “Calibration System for Robot Production Control and Accuracy”, In : Robot Calibration, Bernhardt and Albright, pp. 37-56, Chapman & Hall, ISBN 0 412 49140 0, Cambridge, UK.

Altera: www.altera.com (accessed in May 2009).

Andraka, R., A survey of CORDIC algorithms for FPGAs., 1998, Proceedings of the 1998 ACM/SIGDA sixth international symposium on Field Programmable Gate Arrays, Monterey, CA. pp.191-200

Arndt, R. E. A., 1981, “Recent Advances in Cavitation Research”, In: Advances in Hydroscience, Vol. 12, Academis Press, New York, p.p. 1-72.

Baker, D.R., 1990, “Some topological problems in robotics”, The Mathematical Intelligencer, Vol.12, No.1, pp. 66-76.

Dennis JE, Schnabel RB. Numerical Methods for Unconstrained Optimisation and Non-linear Equations, New Jersey:Prentice-Hall, 1983.

Ecober, X., Egusquiza, E., Farhat, M., Avellan, F., Coussirat, M., 2006, “Detection of Cavitation in Hydraulic Turbines”, Mechanical Systems and Signal Processing, Vol. 20, Issue 4, p.p.- 983-1007.

Ginani, L. and Motta, J. M S. T.., 2007, “A Laser Scanning System for 3D Modeling of Industrial Objects Based on Computer Vision”, Proceedings of 19th International Congress of Mechanical Engineering, Vol. 1, Brasilia-DF, Brazil, 10 p.

Gottlieb, D.H., 1986, “Robots and Topology”, Proceedings of the IEEE International Conference on Robotics and Automation, pp. 1689-1691.

Hammit, F. G., 1979, “Cavitation erosion: the state-of-the-art and predicting capability”, Applied Mechanics Reviews, Vol. 32, 6, p.p. 665-675.

Hollerbach, J. M., Benett, D. J., 1988, “A Survey of Kinematic Calibration”, Robotics Review, pp. 207-242.

Li, S.C. (editor), 2000, “Cavitation of Hydraulic Machinery”, Vol. 1, Imperial College Press, London.

J. Becker and R. W. Hartenstein, 2003, Configware and morphware going mainstream, Journal of Systems Architecture 49:127-142.

Jacoby, S.L.S, Kowalik, J.S. and Pizzo, J.T., 1972, “Iterative Methods for Nonlinear Optimization Problems”, Prentice Hall, New Jersey, USA, 274 p.

Kung,Y., Tseng, K., Sze, H.,Wang, A., 2006, FPGA-Implementation of Inverse Kinematics and Servo Controller for Robot Manipulator. Proceedings of the 2006 IEEE. International Conference on Robotics and Biomimetics, China, 2006. pp. 1163- 1168

McKerrow, P. J., 1995, "Introduction to Robotics", 1st ed., Ed. Addison Wesley, Singapore, 800 p.

Motta, J.M.S.T., 2005, “An Investigation of Singularities in Robot Kinematic Chains Aiming at Building Robot Calibration Models for Off-line Programming”, Journal of the Brazilian Society of Mechanical Sciences and Engineering, Vol. 2, No. 2, pp. 200-204.

Motta, J.M.S.T., 2007, “Robot Calibration: Modeling, Measurement and Applications”. In: Industrial Robotics: Programming, Simulation and Applications, Low Kin-Huat. (Org.), 1st ed., v. 1, pp. 107-130, Mammendorf - Germany: Verlag Robert Mayer-Scholz, ISBN 3-86611-286-6, Croatia.

Parmar, R. S., 1997, “Welding Processes and Technology”, 2nd Ed. Khanna Publishers: Delhi.

Paul, R. P., 1981, "Robot Manipulators - Mathematics, Programming, and Control", Boston, MIT Press, Massachusetts, USA, 279 p.

Schröer, K., 1993, “Theory of Kinematic Modelling and Numerical Procedures for Robot Calibration”, In: Robot Calibration, Ed. Chapman & Hall, pp. 157-193.

Schröer, K., Albright, S. L. and Grethlein, M., 1997, “Complete, Minimal and Model-Continuous Kinematic Models for Robot Calibration”, Robotics & Computer-Integrated Manufacturing, Vol. 13, No. 1, pp. 73-85.

Turbine Repair, 2000, “Facilities Instructions, Standards, & Techniques”, USA Department of Interior Bureau Reclamation In: http://www.usbr.gov/power/data/fist/fist2_5/vol2-5.pdf. (accessed in June, 2008).

Xilinx: www.xilinx.com (accessed in June of 2008).

8. RESPONSIBILITY NOTICE

The authors are the only responsible for the printed material included in this paper.